



## A review of the elemental composition and redox conditions of Oligocene organic matter-rich deposits, Western Anatolia Turkey

D. B. Koralay<sup>1,a</sup>

<sup>1</sup>Pamukkale University, Geological Engineering Denizli, Turkey.

Accepted 13 May 2018

### Abstract

Organic matter-rich deposits of the Oligocene Hayrettin Formation, Denizli, West of Turkey, may be considered as a carbonaceous interval within a succession dominated by mudstone and sandstone. Samples were investigated to determine the source rock composition and provenance, and redox conditions of the depositional environment. Carbonaceous rocks are characterized by high organic carbon (2.12-34.35 wt. %) contents and by significant enrichments of several trace elements (Co, Cr, Mo, Ni, Pb, S, Th, U and V) relative to average shale. According to La/Th versus Hf diagram, Al<sub>2</sub>O<sub>3</sub>/TiO<sub>2</sub> ratios, and Cr/Ni, Th/Co, Th/Cr, and Cr/Th ratios indicate that the sediment was derived from intermediate source rocks in addition to being an important contribution of detritus. Average CIA, PIA and CIW values imply intense weathering of the source terrane. K<sub>2</sub>O/Na<sub>2</sub>O, SiO<sub>2</sub>/Al<sub>2</sub>O<sub>3</sub> and K<sub>2</sub>O/Na<sub>2</sub>O ratios and bivariate discriminant functions diagram indicate that most samples in the active continental margin. Ni/Co, V/Cr, and U/Th ratios of the studied samples suggest that the redox conditions of depositional environment are oxic.

*Keywords:* Carbonaceous Rock; Hayrettin Formation; provenance; weathering; redox condition.

### 1. Introduction

The study area is located 70 km northeast of the Denizli province (southwest of the Turkey) (Figure 1). Study materials consist of carbonaceous rocks that are sedimentary rocks, enriched with organic carbon. The average amount of organic matter in mudrock is about 2.1 weight percent, in limestone is about 0.29 percent, and in sandstone is about 0.05 percent, and other organic-rich rocks typically contain 3 to 10 or more percent by weight of organic matter [1-3]. General properties of carbonaceous sediments which are rich in organic matter can be black colored, opaque, solid, and compact. Even though carbonaceous rocks make only a small part of sedimentary rocks, they are important hydrocarbon sources and can also be enriched with certain trace elements (Co, Cr, Cu, Mo, Ni, and V) as well as enriched organic matter [4-6].

Detailed studies which are purposes of geology, petrography, morphological features and tectonic setting, and prospective were carried out around the study area [7-12]. Although research on organic and inorganic geochemistry of organic matter rich rocks and Tertiary coals in Turkey [6, 13, 14]. There are no studies in the literature on elemental characterization and redox conditions of the carbonaceous rocks from Oligocene Hayrettin Formation. This paper investigated organic-rich samples collected from the Hayrettin Formation (Denizli/Western Anatolia, Turkey) to determine the redox conditions of their depositional environment. Additionally, weathering effects, source rock composition and provenance characteristics, and trace element enrichments of the carbonaceous rocks are addressed.

### 2. Field observations

Study area contains rock assemblages, which are organic matter-rich claystone, mudstone, sandstone and coaly carbonaceous shales, and it is located to the east of Denizli province in the Aegean region (Western Anatolia, Turkey) (Figure 1). Basement rocks of the study area, which include Middle Triassic metamorphic rocks such as meta

conglomerates, quartzite, quartzite schist and schist, are overlain by Late Triassic dolomites and dolomitic limestones. The Oligocene Hayrettin Formation of the Denizli Basin (Western Anatolia, Turkey) is interpreted to have accumulated as lagoon/tidal flat deposits, reef deposits, and fine grained shelf deposition [9]. The reef deposits that comprise the

<sup>a</sup> Corresponding author;

Phone: +90-258-296-3377, Email: [dbkoralay@pau.edu.tr](mailto:dbkoralay@pau.edu.tr)

lower part of the formation are referred to as the Sarıkavak Reef Member and the southeastern shelf transition zones and shelf deposits are named as the Dazkırı Member. These rocks accumulated in shallow shelf environment [9]. The dominant rock type of the Hayrettin Formation is sandstone containing intercalated conglomerate and lignite-

bearing mudstone. Sandstones are generally yellowish-brown, and grain size ranging from fine sand to coarse sand, and medium to thick bedded. Sandstone layers contain calcite-filled vertical (relative to layering) fractures. Carbonaceous rocks are laterally discontinuous and their lateral thickness is variable.

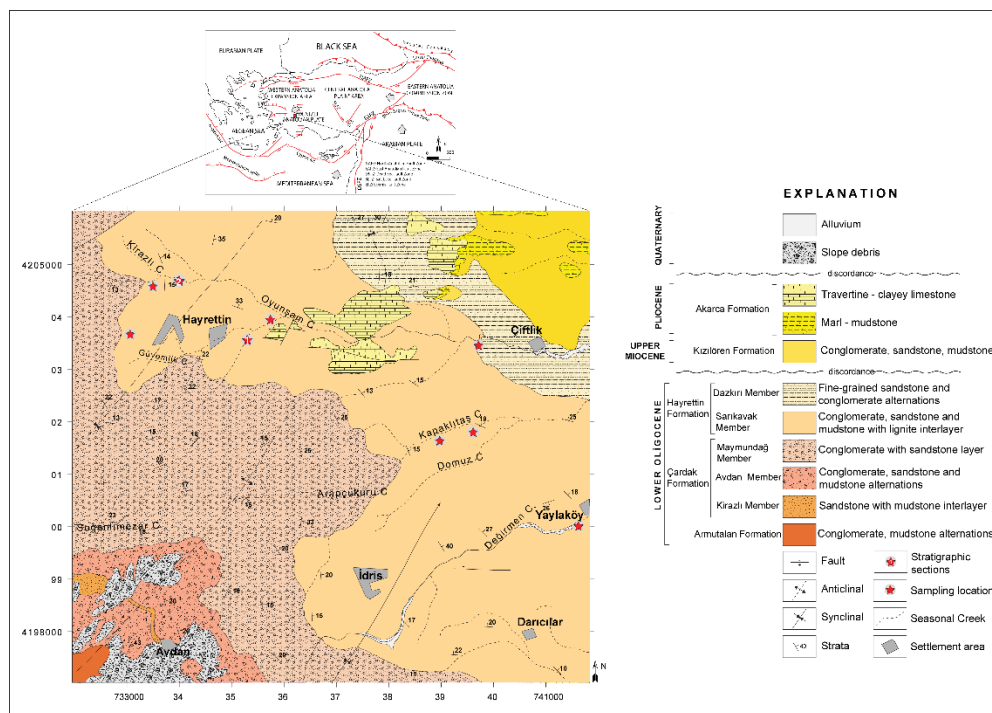


Figure 1. (a) Geological map of Hayrettin region (Denizli/Western Anatolia, Turkey) (Modified from [9]).

### 3. Sampling and analytical procedures

Total fifty-one carbonaceous rock samples were collected from fresh outcrops of the Hayrettin Formation. Seventeen of these samples belong to two sections of the Hayrettin Formation. Trace elements for these samples were analyzed by Spectro XLAB-2000 Polarized Energy Dispersive X-ray fluorescence (PEDXRF) spectrometer (Ankara University). The mineralogical composition of the four samples was determined by XRD, using an Inel Equinox 1000 analyzer with Co-K $\alpha$  radiation (Ankara University). The instrument was operated at the following settings; 60 mA, 60 kV (Option :30

kV) generator and Co radiation X-ray tube was used as X-ray source. Quanta 250 FEG series from FEI instrument was used to obtain SEM photomicrograph and EDS spot analysis datas to investigate the surface images and compositional features of the minerals (Aksaray University). Analysis of total organic carbon (TOC, wt.%) was carried out on a Rock Eval-6 (RE-6) instrument equipped with a TOC module using the IFP 160000 (Institut Francais du Petrole) standard in the Research Centre Laboratories of Turkish Petroleum Corporation (TPAO).

### 4. Results

#### 4.1. Elemental and mineralogical composition of carbonaceous rocks

The strong positive correlation ( $r = 0.83$ ) of Al<sub>2</sub>O<sub>3</sub> and TiO<sub>2</sub> suggests that Ti is contained mainly in phyllosilicates [15] (Table 1). This correlation also

reflect the sympathetic relationship of clay flux (reflected by Al) with coarser clastic sediment (reflected in Ti abundance).

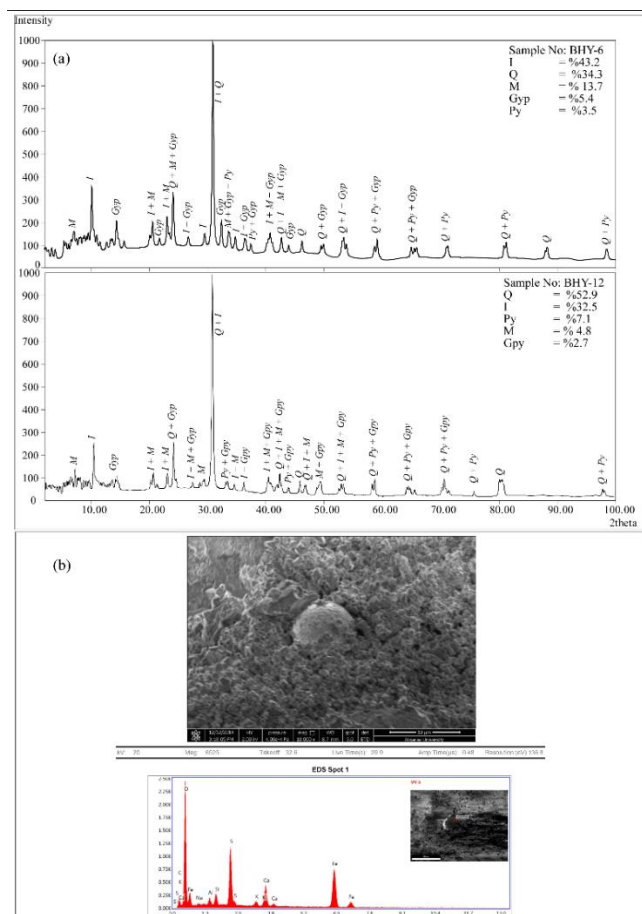


Figure 2. (a) X-ray diffraction patterns and mineralogical composition of carbonaceous rocks, (b) SEM photomicrograph and EDS spot analysis of framboidal pyrite from Hayrettin carbonaceous rocks.

The positive correlations of  $K_2O$  ( $r = 0.93$ ),  $TiO_2$  ( $r = 0.83$ ) with  $Al_2O_3$  and a moderate correlation of  $Na_2O$  with  $Al_2O_3$  ( $r = 0.55$ ) suggest that these elements may be associated with detrital phases. Relatively low concentrations of  $Na_2O$  (0.06 - 0.84%, on average 0.34%) may probably be related to its mobility at the depositional area or to its depletion in the source area by weathering [17]. Clear positive correlation of  $Al_2O_3$  ( $r = 0.93$ ), Th ( $r = 0.76$ ) and Rb ( $r = 0.95$ ) with  $K_2O$  suggesting that the concentrations of these elements are controlled by the abundance of illite [18]. Clay mineralogy of an analyzed sample can be revealed by  $K_2O/Al_2O_3$  [16]. It is possible to make inferences regarding changes in the relative abundances of kaolinite (Al) and illite (K).  $K_2O/Al_2O_3$  of the studied samples varies from 0.02 to 0.21 wt. %, which indicate that illite is the dominant clay mineral in these carbonaceous rocks (Figure 2a). Very low correlations of  $Fe_2O_3$  and  $MgO$  with  $Al_2O_3$  ( $r^2 = 0.04$  and  $0.17$ , respectively) suggest that the abundances of Mg are not controlled by aluminous phases. The poor correlation of Fe and Al may reflect the fact that the Fe was taken up by sulfate reduction (and consequent generation of

hydrogen sulfide) in the early diagenetic history of these deposits. The index of compositional variability ( $ICV = (Fe_2O_3 + K_2O + Na_2O + CaO + MgO + MnO)/Al_2O_3$ ) is a measure of the quantity of clay minerals relative to the silicate minerals in a rock. ICV values of carbonaceous rocks range from 0.50 to 3.11 (Table 1) suggesting that most samples may also compositionally contain rock forming minerals in addition to clay minerals [16]. Ba, Sr and Th show positive correlations with  $Al_2O_3$  ( $r = 0.87$ ,  $r = 0.43$  and  $r = 0.75$ , respectively) indicating the concentrations of these large-ion lithophile elements (LILE) are controlled by clay flux. High field-strength elements (HFSE) are enriched in felsic rocks and reflect provenance compositions [19]. Co, Ni and V concentrations against  $Al_2O_3$  ( $r = -0.12$ ,  $r = -0.11$ , and  $r = 0.09$ , respectively) suggesting that the concentrations of these elements reflect contributions from more than one mineral in addition to clay minerals [15]. Quartz, illite, montmorillonite, gypsum, and pyrite dominate the mineralogy of the studied samples (Figure 2a). Quartz is the dominant constituent of all studied samples (31.9 - 58.6 wt.%). Gypsum (2.7 - 6.5 wt.%) occurs as a crack-filling

mineral in the Hayrettin Formation carbonaceous rocks and it was probably precipitated primarily as a metal sulfide by sulfate reducing bacteria under relatively reducing conditions. Pyrite varies from 1.6 to 7.1 % in three analyzed samples. SEM analysis of Hayrettin samples reveals the presence of pyrite

framboids (Figure 2b). The pyrite might be produced as a result of bacterial sulfate reduction in the Hayrettin Formation. According to the XRD graphics the presence of illite and montmorillonite may be related to mica minerals derived from the source area.

Table 1. Minimum and maximum values of total organic carbon (TOC.wt.%), trace and major element composition and some ratios of the carbonaceous rocks from Hayrettin Formation, Western Anatolia.

Element (n=51)	Min	Max	Average	Element (n=51)	Min	Max	Average
TOC (wt.%)	0.21	39.61	9.73	Rb (ppm)	3.20	178.4	117.34
SiO <sub>2</sub>	18.59	56.44	41.85	S (%)	0.20	6.54	2.13
TiO <sub>2</sub>	0.04	1.13	0.79	Sr (ppm)	67.00	271.0	146.98
Al <sub>2</sub> O <sub>3</sub>	3.19	21.30	14.28	Ta (ppm)	3.80	9.10	5.97
Fe <sub>2</sub> O <sub>3</sub>	1.69	8.61	5.64	Th (ppm)	1.00	16.90	10.68
MgO	0.31	3.73	1.68	U (ppm)	6.10	61.40	15.82
CaO	0.20	22.59	3.75	V (%)	38.00	234.0	164.61
Na <sub>2</sub> O	0.06	0.84	0.34	Zn (ppm)	9.00	102.0	45.89
K <sub>2</sub> O	0.07	3.91	2.59	Zr (ppm)	8.30	280.0	178.37
Al <sub>2</sub> O <sub>3</sub> /TiO <sub>2</sub>	13.33	83.95	19.26	Cr/Ni	0.62	12.01	4.29
Al <sub>2</sub> O <sub>3</sub> +K <sub>2</sub> O+Na <sub>2</sub> O	3.32	26.05	17.21	Cr/Th	14.19	118.98	28.25
K <sub>2</sub> O/Al <sub>2</sub> O <sub>3</sub>	0.02	0.21	0.18	La/Th	1.93	31.40	4.02
K <sub>2</sub> O/Na <sub>2</sub> O	1.08	29.51	12.91	Ni/Co	0.97	8.42	2.92
SiO <sub>2</sub> /Al <sub>2</sub> O <sub>3</sub>	2.19	13.09	3.11	Rb/Sr	0.03	1.94	0.88
ICV	0.50	3.81	1.12	Th/Co	0.04	0.71	0.38
Al (%)	1.69	11.27	7.56	Th/Cr	0.01	0.07	0.04
Ba (ppm)	20.50	728.70	426.75	Th/U	0.02	2.09	0.97
Co (ppm)	18.60	64.90	31.43	U/Th	0.48	45.3	2.43
Cr (%)	119.0	442.0	272.69	V/Cr	0.29	1.18	0.64
Cu (ppm)	10.90	97.40	32.32	molAl <sub>2</sub> O <sub>3</sub>	0.03	0.21	0.14
Fe (%)	1.18	6.02	3.94	molCaO*	0.001	0.026	0.00
Hf (ppm)	3.00	8.70	5.30	mol(CaO* + Na <sub>2</sub> O)	0.00	0.04	0.01
La (ppm)	24.70	57.80	36.16	molK <sub>2</sub> O	0.01	0.04	0.03
Mg (%)	0.18	2.25	1.02	molNa <sub>2</sub> O	0.001	0.014	0.01
Mo (ppm)	2.60	72.30	18.71	CIA (%)	72.01	92.02	79.33
Nb (ppm)	2.10	27.30	18.69	PIA (%)	80.91	98.34	92.09
Ni (ppm)	24.00	255.1	91.62	CIW (%)	84.12	98.70	93.53
Pb (ppm)	7.60	36.40	23.51				

**Note:** Major elements in oxide: %. n: sample number. min: minimum values. max: maximum values. ICV ( $Fe_2O_3 + K_2O + Na_2O + CaO + MgO + TiO_2$ )/ $Al_2O_3$  [16], mol: Major element composition of studied samples in molar proportions, CIA = Chemical Index of Alteration [22]; PIA = Plagioclase Index of Alteration [ $(Al_2O_3 - K_2O)/((Al_2O_3 - K_2O) + CaO^* + Na_2O)$ ] x 100 [24]; CIW = Chemical Index of Weathering [ $(Al_2O_3/(Al_2O_3 + CaO^* + Na_2O))$ ] x 100 [25], CaO\* = CaO in silicate fraction.

#### 4.2. Weathering effects

The Th/U versus Th plot for the Hayrettin Formation carbonaceous rocks plots in the field of depleted mantle rocks (Figure 3). In addition, samples also show limited degree of weathering trend [20]. The positive correlations between Al<sub>2</sub>O<sub>3</sub> and TiO<sub>2</sub>, K<sub>2</sub>O (r = 0.83, r = 0.93, respectively) suggest that Al and Ti and Al and K behaved similarly as might be expected of two detrital components and also positive correlation between the K<sub>2</sub>O-Ba (r = 0.96) in studied samples indicated that effect of chemical weathering [21]. The chemical index of alteration (CIA) is used to characterize the degree of weathering in

provenance areas. CIA is calculated as follows; CIA =  $(Al_2O_3/(Al_2O_3 + CaO^* + Na_2O + K_2O))$  x 100 [22]. The CIA value of the studied samples varies from 72.01 to 92.02, suggesting relatively intensive chemical weathering in the source area (Table 1). Due to the intensive chemical weathering, Na<sub>2</sub>O and CaO in samples are almost leached out. In Al<sub>2</sub>O<sub>3</sub>, Na<sub>2</sub>O, CaO\* (CaO in silicate fraction) and K<sub>2</sub>O in A-CN-K (A = Al<sub>2</sub>O<sub>3</sub>, CN = CaO\* + Na<sub>2</sub>O, K = K<sub>2</sub>O) ternary diagram [23], samples are showed almost parallel to the weathering trend (Figure 4).

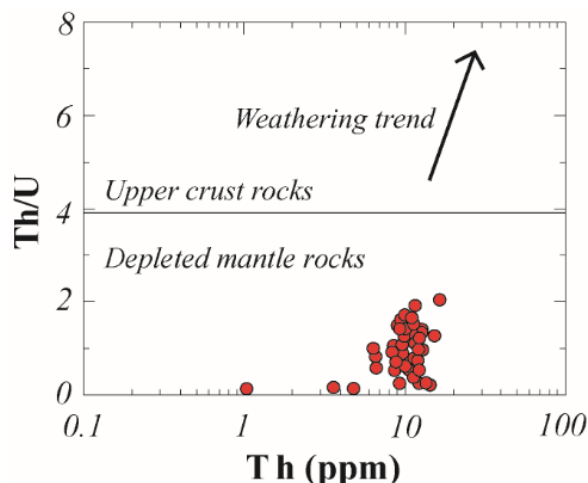


Figure 3. Plots of Th/U versus Th of the studied samples (modified from [20]).

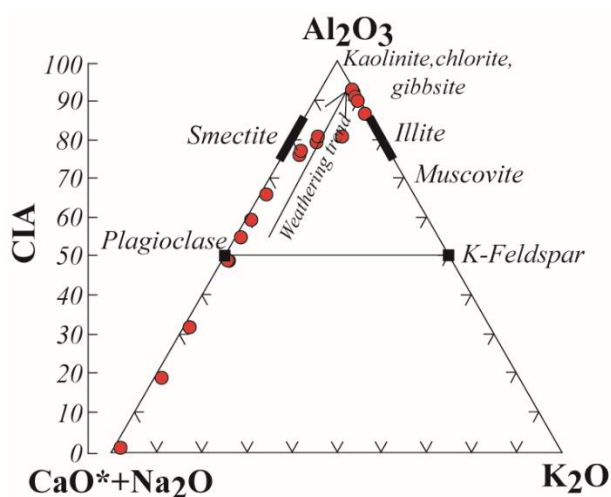


Figure 4. A-CN-K ternary diagram showing weathering trend. A =  $\text{Al}_2\text{O}_3$ , CN =  $\text{CaO}^* + \text{Na}_2\text{O}$ , K =  $\text{K}_2\text{O}$  (all in molar proportions).  $\text{CaO}^*$  = CaO content of silicate fraction (after [23]).

Plagioclase index of alteration (PIA) values, which indicate the intensity of alteration of source material [24], varies from 80.91 to 98.39 % and chemical index of weathering (CIW) values, which indicate the degree of source weathering [25] varies from 84.12 to 98.70 % in samples (Table 1). Average PIA and

CIW values indicate relatively higher degree of weathering than calculate from CIA values. Average Rb/Sr ratio (0.88) (Table 1) is very close to the average Post Archean Australian Shale composition (0.80) and this may indicate that the degree of source area weathering was relatively intense [26].

## 5. Discussion

### 5.1. Source rock composition and provenance

In the studied samples, the  $\text{Al}_2\text{O}_3/\text{TiO}_2$  ratio ranges from 13.33 to 22.36 suggesting derivation from intermediate rocks [27]. According to the La/Th versus Hf diagram [28] (Figure 5a), most of the samples display nearly vertical orientation which is pointing mixed felsic-basic source, which include metamorphic rocks in addition to being an important contribution of detritus. On the discrimination

diagram for sedimentary provenance [29], studied samples plot on the quartzose sedimentary provenance and mafic igneous provenance fields (Figure 5b). In ultramafic rocks, Cr/Ni ratio is about 1.6, and the Cr/Ni ratios of the studied samples range from 0.74 to 12.01 (average = 4.29) (Table 1), which are indicate that these samples may derived from intermediate source rocks [30]. The Th/Co, Th/Cr

and Cr/Th ratios of the studied carbonaceous rocks range from 0.07 – 0.71, 0.02 – 0.07 and 14.19 – 118.98, respectively. These ratios are compared with those of sediments derived from felsic and mafic rocks which indicate that studied samples are

between both rock types [16, 31]. On the  $K_2O/Na_2O$  versus  $SiO_2$  and  $SiO_2/Al_2O_3$  versus  $K_2O/Na_2O$  diagrams most samples from the Hayrettin Formation plot in the active continental margin field [32, 33], (Figure 5c and 5d).

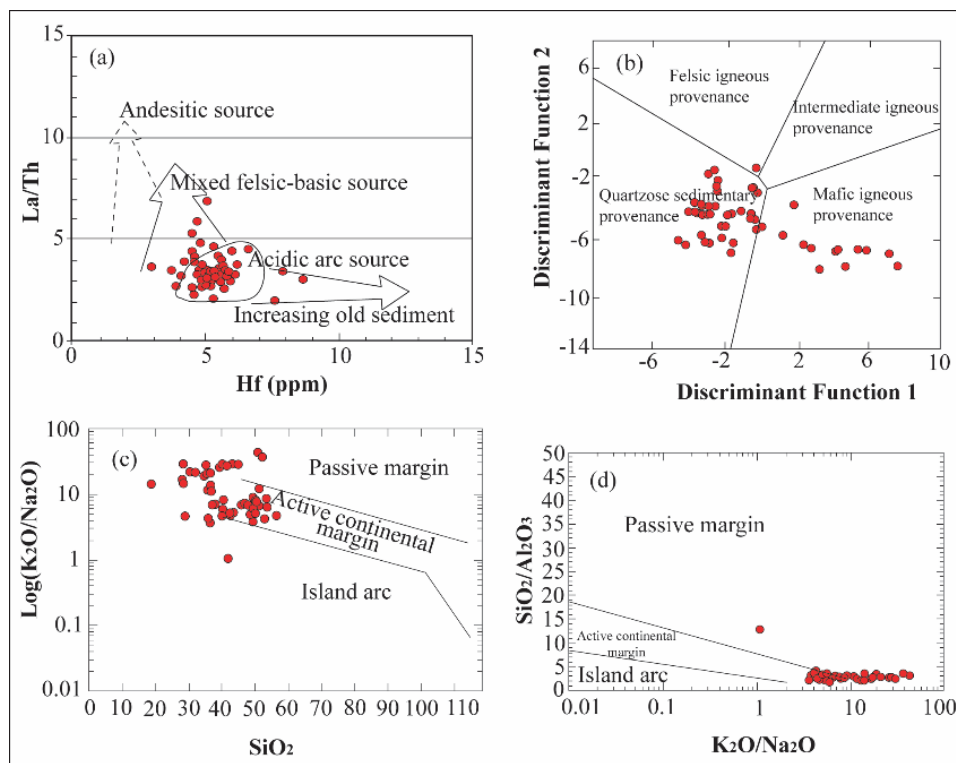


Figure 5. Discrimination diagrams for composition and provenance signature of studied samples using (a) La/Th versus Hf plot for discriminating source rocks sedimentary rocks (compositional fields of the source rock after [28]), (b) major elements (after [29]). The discriminant function is as follows: Discriminant Function 1 =  $(-1.773 \times TiO_2) + (0.607 \times Al_2O_3) + (0.76 \times Fe_2O_3) + (-1.5 \times MgO) + (0.616 \times CaO) + (0.509 \times Na_2O) + (-1.22 \times K_2O) + (-9.09)$ . Discriminant Function 2 =  $(0.445 \times TiO_2) + (0.07 \times Al_2O_3) + (-0.25 \times Fe_2O_3) + (-1.142 \times MgO) + (0.438 \times CaO) + (0.432 \times Na_2O) + (1.426 \times K_2O) + (-6.861)$ , (c) Tectonic discrimination diagrams for sedimentary rocks, (d)  $K_2O/Na_2O$  versus  $SiO_2$ . Tectonic lines are after [33] and (b)  $SiO_2/Al_2O_3$  versus  $K_2O/Na_2O$ . Tectonic lines are after [32].

## 5.2. Geochemical approach to depositional environment

Total organic carbon (TOC, %) contents of Hayrettin Formation carbonaceous rocks on average 9.73 wt.%. All the samples have rich source rock quality (Table 1). Ni/Co ratios of the carbonaceous samples range from 0.97 to 8.42, and it usually indicates deposition under oxic conditions [34], (Figure 6a). V/Cr ratios of the studied samples range from 0.29 to 1.18 suggesting deposition under oxic conditions [35], (Figure 6b). U/Th ratios less than 1.25 indicate well-oxygenated conditions, whereas values above 1.25 indicate suboxic and anoxic conditions [34]. U/Th ratios of the studied samples generally less than 1.25

pointing to oxic depositional conditions (Figure 6c).

The authigenic uranium content is also taken into account as a redox indicator of the depositional environment and calculated as; authigenic U =  $(Total\ U) - Th/3$  [36]. Some major element contents of sedimentary rocks provide useful information on climatic conditions in the source area. On the binary  $SiO_2$  versus  $(Al_2O_3 + K_2O + Na_2O)$  diagram [37] studied samples plot in the semiarid climate field (Figure. 7).

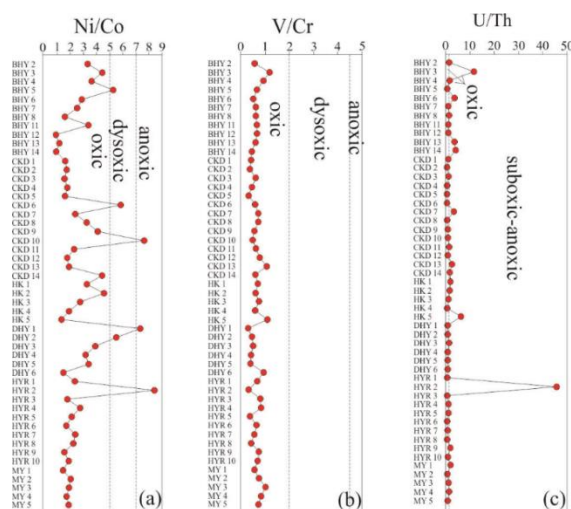
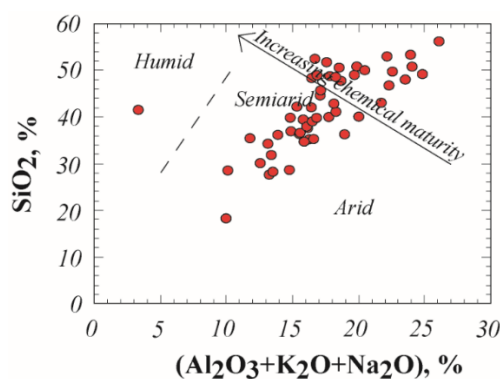


Figure 6. Paleoredox conditions of the carbonaceous rocks.

Figure 7. Bivariate  $\text{SiO}_2$  versus  $(\text{Al}_2\text{O}_3 + \text{K}_2\text{O} + \text{Na}_2\text{O})$  paleoclimate discrimination diagram. Fields after [37].

### 5.3. Chemical components and trace element enrichments of carbonaceous rocks

Trace element enrichments in carbonaceous rocks have been compared to trace element contents of the certain reducing environments and the enrichment factors (EF) have been calculated using;  $EF_{\text{element}} = (\text{element}/\text{Al})_{\text{sample}} / (\text{element}/\text{Al})_{\text{average shale}}$  [38] (Table 2). Considering the  $\text{Al}_2\text{O}_3$  (clay minerals),  $\text{SiO}_2$  (silicate minerals) and  $\text{CaO}$  (carbonate minerals) contents, these three of the major chemical components indicate that the analyzed carbonaceous rocks are compositionally similar to the average shale [39]. Compared to average shale, Hayrettin carbonaceous rocks are characterized by more pronounced TOC ( $EF_{\text{TOC}} = 80.48$ ), sulfur ( $EF_{\text{S}} = 15.10$ ), Co ( $EF_{\text{Co}} = 2.11$ ), Cr ( $EF_{\text{Cr}} = 3.67$ ), Mo ( $EF_{\text{Mo}} = 23.50$ ), Ni ( $EF_{\text{Ni}} = 1.85$ ), Pb ( $EF_{\text{Pb}} = 1.27$ ), Th ( $EF_{\text{Th}} = 1.04$ ), U ( $EF_{\text{U}} = 6.24$ ) and finally V ( $EF_{\text{V}} = 1.52$ ) enrichments. Total sulfur (TS) contents of the studied samples range from 0.68 to 6.54 %. The amount of S in a sedimentary deposits can be

affected by the amount of available reactive Fe in that environment. Sulfur and organic carbon in studied samples show a strong positive correlation ( $r^2 = 0.81$ ,  $n = 11$ ). One could argue that enhanced C abundances increase the rate of bacterial sulfate reduction that produces large amounts of  $\text{H}_2\text{S}$ , which, in the presence of reactive Fe, yields pyrite. Higher supply of organic matter, higher sulfur concentration result in relatively anoxic conditions which formation of pyrite mineral and XRD characteristics of the samples were supported these results (Figure 2a). As stated above, high amounts of organic matter preserved under anoxic pore water conditions favor bacterial sulfate reduction and the consequent generation of hydrogen sulfide. If enough reactive Fe is present, pyrite will form. On the other hand, under Fe-limited conditions, very little pyrite may form in the samples from Hayrettin Formation.

Table 2. Enrichment factors (EF) for total organic carbon (TOC), sulfur and several trace element contents of Hayrettin carbonaceous rocks in comparison to average shale, Mediterranean sapropels, Monterey Formation, Namibian mud lens, Gulf of California and Peru margin.

Element	Hayrettin Carbonaceous Rocks	Average Shale*	EF	Mediterranean Sapropels**	EF	Monterey Formation***	EF	Namibian Mud Lens**	EF	Gulf of California**	EF	Peru Margin**	EF
<b>TOC</b>	9,73	0.20	80,48	6.91	1,07	5.02	1.62	5.37	0,43	4.35	6,16	8.33	1,03
<b>S</b>	2,13	0.20	15,10	3.26	0,43	nd	nd	1.20	0,36	0.56	8,98	1.43	1,13
<b>Ba</b>	426,75	580.00	0,84	228.00	0,99	363.00	0,68	324.00	0,22	566.00	1,44	314.00	0,83
<b>Co</b>	31,43	19.00	2,11	68.00	0,27	6.00	3,39	3.50	1,63	6.60	10,12	6.10	3,50
<b>Cr</b>	273	90.00	3,67	110.00	1,38	139.00	1,20	83	0,57	44.00	12,49	98.00	1,79
<b>Cu</b>	32,32	45.00	0,97	127.00	0,16	45.00	0,49	37.00	0,17	27.00	2,70	49.00	0,48
<b>Mo</b>	18,71	1.00	23,50	105.00	0,10	20.00	0,60	40.00	0,08	12.00	3,26	42.00	0,30
<b>Ni</b>	91,62	68.00	1,85	208.00	0,28	104.00	0,61	46.00	0,39	38.00	5,52	74.00	0,91
<b>Pb</b>	23,51	22.00	1,27	11.30	1,14	6.00	2,36	4.50	0,89	17.00	2,74	18.00	0,83
<b>Th</b>	10,68	12.00	1,04	nd	nd	nd	nd	nd	nd	nd	nd	nd	nd
<b>U</b>	15,82	3.70	6,24	15.50	0,69	nd	nd	30.00	0,11	5.70	6,75	10.50	1,17
<b>V</b>	165	130.00	1,52	518.00	0,18	265.00	0,38	138.00	0,20	101.00	3,26	152.00	0,69
<b>Zn</b>	45,89	95.00	0,61	96.00	0,28	145.00	0,20	35.00	0,24	88.00	1,09	106.00	0,29

*Note: TOC and S in percent (%); minor elements in ppm; nd = not detected. \*Average shale data from [39]. \*\*Mediterranean sapropels, Namibian Mud Lens and Gulf of California data from [5]. \*\*\*Monterey Formation data from [40].*

## 6. Conclusions

Average CIA, PIA and CIW values of the samples indicate intensive weathering in the source area. According to ICV values and major and certain trace elements of carbonaceous rocks suggest that these samples are derived from the intermediate rocks. This paper has also presented successful applications of the XRD, XRF and total organic carbon analysis to the determination of redox conditions of carbonaceous rocks. One of the principal results of this conclusion is that Ni/Co, V/Cr, and U/Th ratios can allow us to identify oxic depositional conditions. The presence of pyrite and a strong positive

correlation between the total sulfur and organic carbon may indicate that anoxic conditions were dominate from time to time. In comparison with average shale, carbonaceous rocks are enriched TOC, sulfur, Co, Cr, Mo, Ni, Pb, Th, U and finally V. These elements may be transported to the sediment with the clay minerals and distribution of these elements in the carbonaceous rocks may be derived from the basement rocks of the study area, which include metamorphic rocks in addition to being an important contribution of detritus.

## Acknowledgements

This research was financially supported by the TÜBİTAK (The Scientific and Technological Research Council of Turkey) Foundation (project number: 110Y356). The author would like to thanks Y.K. Kadioğlu (University of Ankara) for their

contribution to the analytical procedures. Thanks are due to T. Koralay (University of Pamukkale) for their contribution to the field studies and K. Deniz (University of Ankara) and B. Güllü (University of Aksaray) for helps during XRF and SEM analysis.

Average CIA, PIA and CIW values of the samples **References**

- [1] Hunt, J.M. Petroleum geochemistry and geology, 2nd ed. W.H. Freeman and Company New York 1996.
- [2] Boggs, S. Petrology of sedimentary rocks, 2nd ed. Cambridge University Press England 2009.
- [3] Mendonça, Filho, J.G., Sommer, M.G., Klepzig, M.C., Mendonça, J.O., Silva, T.F., Kern, M.L., Menezes, T.R., Jasper, A., Silva, M.C., Santos, L.G.C. Permian carbonaceous rocks from the Bonito Coalfield, Santa Catarina, Brazil: Organic facies approaches, *International Journal of Coal Geology* 2013; 111: 23-36.
- [4] Lipinski, M., Warning, B., Brumsack, H.J. Trace metal signatures of Jurassic/Cretaceous black shales from the Norwegian Shelf and the Barents Sea, *Palaeogeography, Palaeoclimatology, Palaeoecology* 2003; 190: 459-475
- [5] Brumsack, H.J. The trace metal content of recent organic carbon-rich sediments: Implications for Cretaceous black shale formation, *Palaeogeography, Palaeoclimatology, Palaeoecology* 2006; 232: 344-361
- [6] Sarı, A., Çılsal, M., Koç, S. Element enrichments in bituminous rocks, Hatlıdağ field, Göynük/Bolu, *Bulletin of Mineral Research and Exploration* 2015; 150: 109-120
- [7] Ercan, T., Güney, E., Baş, H. Denizli volkanitlerinin petrolojisi ve plaka tektoniği açısından bölgesel yorumu, *Türkiye Jeoloji Kurumu Bülteni* 1983; 26 (2), 153-159
- [8] Okay, A.İ. Denizli' nin güneyinde Menderes Masifi ve Likya Napılarının jeolojisi, *Maden Tetkik ve Arama Dergisi (in Turkish)* 1989; 109, 45-58
- [9] Göktaş, F., Çakmakoğlu, A., Tarı, E., Sütçü, F.Y., Sarıkaya, H. Çivril-Çardak arasındaki jeolojisi (in Turkish). General Directorate of Mineral Research and Exploration Technical Report 1989; No. 8701.
- [10] Altunel, E., Hancock, P.L. Morphology and structural setting of Quaternary travertines at Pamukkale, Turkey. *Geological Journal* 1993; 28(3-4): 335-346.
- [11] İslamoğlu, Y., Atay, G., Gedik, F., Aydın, A., Hakyemez, A., Babayigit, S., Sarıkaya, H. Batı Toroslardaki Denizel Oligo-Miyosen Çökellerinin Biyostratigrafisi (Denizli). *Maden Tetkik ve Arama Genel Müdürlüğü Jeoloji Etütleri Dairesi Ankara* 2005; Rapor no. 10763.
- [12] Koralay, O.E., Candan, O., Akal, C., Dora, O.Ö., Chen, F., Satır, M., Oberhanslı, R. Menderes Masifindeki Pan Afrikan ve Triyas yaşlı metagranitoidlerin jeolojisi ve jeokronolojisi, Batı Anadolu, *Türkiye. MTA Dergisi* 2011; 142, 69-121.
- [13] Karayigit, A.İ., Akgün, F., Gayer, R.A., Temel, A. Quality, palynology, and palaeoenvironmental interpretation of the Ilgın

- lignite, Turkey. *Inter Jour Coal Geol* 1999; 38: 219–236.
- [14] Korkmaz, S., Kara Gülbay, R. Organic geochemical characteristics and depositional environments of the Jurassic coals in the western Taurus of southern Turkey. *International Journal of Coal Geology* 2007; 70 (4), 292–304.
- [15] Condie, C.K., Noll, Jr., P.D., Conway, C.M. Geochemical and detrital mode evidence for two sources of Early Proterozoic sedimentary rocks from the Tonto Basin Supergroup, Central Arizona. *Sedimentary Geology* 1992; 77: 51-76.
- [16] Cox, R., Low, D.R., Cullers, R.L. The influence of sediment recycling and basement composition on evolution of mudrock chemistry in the southwestern United States. *Geochimica et Cosmochimica Acta* 1995; 59: 2919-2940.
- [17] Asiedu, D.K., Suzuki, S., Nogami, K., Shibata, T. Geochemistry of Lower Cretaceous sediments, Inner Zone of Southwest Japan: Constraints on provenance and tectonic environment. *Geochemical Journal* 2000; 34: 155-173.
- [18] Nagarajan, R., Madhavaraju, J., Nagendra, R., Armstrong-Altrin, J.S., Moutte, J. Geochemistry of Neoproterozoic shales of the Rabanpalli Formation, Bhima Basin, Northern Karnataka, southern India: implications for provenance and paleoredox conditions. *Revista Mexicana de Ciencias Geológicas* 2007; 24(2): 150-160.
- [19] Taylor, S.R., McLennan, S.M. The continental crust: its composition and evolution. Blackwell Oxford 1985.
- [20] McLennan, S.M., Hemming, S.R., McDaniel, D.K., Hanson, G.N. Geochemical approaches to sedimentation, provenance, and tectonics. In: Johnsson M J, Basu A, eds. *Processes Controlling the Composition of Clastic Sediments*. Geological Society of America Special Paper New York 1993; 21-40.
- [21] Feng, R., Kerrich, R. Geochemistry of fine-grained clastic sediments in the Archean Abitibi greenstone belt, Canada: implications for provenance and tectonic setting. *Geochimica et Cosmochimica Acta* 1990; 54: 1061-1081.
- [22] Nesbitt, H.W., Young, G.M. Early Proterozoic climates and plate motions inferred from major element chemistry of lutites. *Nature* 1982; 299: 715-717.
- [23] Nesbitt, H.W., Young, G.M. Prediction of some weathering trends of plutonic and volcanic rocks based on thermodynamic and kinetic considerations. *Geochimica et Cosmochimica Acta* 1984; 48: 1523-1534.
- [24] Fedo, C.M., Nesbitt, H.W., Young, G.M. Unraveling the effects of K-metasomatism in sedimentary rocks and paleosols with implications for palaeoweathering conditions and provenance. *Geology* 1995; 23: 921-924.
- [25] Harnois, L. The CIW index: a new chemical index of weathering. *Sedimentary Geology* 1988; 55: 319-322.
- [26] McLennan, S.M., Taylor, S.R., Eriksson, K.A. Geochemistry of Archean shales from the Pilbara Supergroup, Western Australia. *Geochimica et Cosmochimica Acta* 1983; 47: 1211-1222.
- [27] Hayashi, K., Fujisawa, H., Holland, H., Ohmoto, H. Geochemistry of ~1.9 Ga sedimentary rocks from northeastern Labrador, Canada. *Geochimica et Cosmochimica Acta* 1997; 61: 4115-4137.
- [28] Floyd, P.A., Leveridge, B.E. Tectonic environment of the Devonian Gramscatho basin, south Cornwall: framework mode and geochemical evidence from turbiditic sandstone. *Journal of the Geological Society of London* 1987; 144: 531-542.
- [29] Roser, B.P., Korsch, R.J. Provenance signatures of sandstone-mudstone suites determined using discriminant function analysis of major-element data. *Chemical Geology* 1988; 67: 119-139.
- [30] Garver, J.I., Scott, T.J. Trace elements in shale as indicators of crustal provenance and terrane accretion in the southern Canadian Cordillera. *Geological Society of America Bulletin* 1995; 107: 440-453.
- [31] Cullers, R.L. The geochemistry of shales, siltstones and sandstones of Pennsylvanian-Permian age, Colorado, U.S.A: implications for provenance and metamorphic studies. *Lithos* 2000; 51: 305-327.
- [32] Maynard, J.B., Valloni, R., Yu, H.S. Composition of modern deep sea sands from arc-related basins. In: Legget J K, ed. *Trench-Forearc Geology: Sedimentation and Tectonics*. London: Geological Society of London Special Publication 1982; 10: 551-561.
- [33] Roser, B.P., Korsch, R.J. Determination of tectonic setting of sandstone-mudstone suites using SiO<sub>2</sub> content and K<sub>2</sub>O/Na<sub>2</sub>O ratio. *Journal of Geology* 1986; 94: 635-650.
- [34] Jones, B., Manning, D.A.C. Comparison of

- geochemical indices used for the interpretation of palaeoredox conditions in ancient mudstones. *Chemical Geology* 1994; 114: 111-129.
- [35] Rimmer, S.M. Geochemical paleoredox indicators in Devonian-Mississippian black shales, Central Appalachian Basin (USA). *Chemical Geology* 2004; 206: 373-391.
- [36] Wignall, P.B., Myers, K.J. Interpreting the benthic oxygen levels in mudrocks, a new approach. *Geology* 1988; 16: 452-455.
- [37] Suttner, L.J., Dutta, P.K. Alluvial sandstone composition and palaeoclimate, I. Framework mineralogy. *Journal of Sedimentary Petrology* 1986; 56(3): 329-345.
- [38] Turgeon, S., Brumsack, H.J. Anoxic vs dysoxic events reflected in sediment geochemistry during the Cenomanian - Turonian Boundary Event (Cretaceous) in the Umbria – Marche Basin of central Italy. *Chemical Geology* 2006; 234: 321-339.
- [39] Wedepohl, K.H. Environmental influences on the chemical composition of shales and clays. In: Ahrens L H, Press F, Runcorn S K, Urey H C, eds. *Physics and Chemistry of the Earth*. Pergamon Oxford Press UK 1971; 305–333.
- [40] Leventhal, J.S. Metal-rich black shales: formation, economic geology and environmental considerations, In: *Shales and Mudstones II*. Schieber, J., Zimmerle, W. And Sethi, P. (eds), Schweizebart' sche Verlagsbuchhandlung Stuttgart 1998; 255-282.